



Contents lists available at ScienceDirect

## Arabian Journal of Chemistry

journal homepage: [www.ksu.edu.sa](http://www.ksu.edu.sa)

# Adenosine and its derivatives improve exercise performance and exert anti-fatigue effects via AMPK/PGC-1 $\alpha$ signaling pathway in mice

Huimin Zhu<sup>a,1</sup>, Tangna Zhao<sup>a,b,1</sup>, Wanbo Zeng<sup>a</sup>, Xiao Dong<sup>a,b</sup>, Yuan Luo<sup>a</sup>, Xiang Li<sup>c</sup>, Aiping Zhang<sup>b,\*</sup>, Weiguo Shi<sup>a,\*</sup>, Liang Xu<sup>a,\*</sup>

<sup>a</sup> State Key Laboratory of Toxicology and Medical Countermeasures, Beijing Institute of Pharmacology and Toxicology, Beijing 100850, PR China

<sup>b</sup> College of Pharmacy, Shanxi Medical University, Taiyuan 030001, PR China

<sup>c</sup> National Resource Center for Chinese Materia Medica, China Academy of Chinese Medical Sciences, Beijing 100007, PR China

## ARTICLE INFO

## Keywords:

Adenosine derivative  
Substitution  
Anti-fatigue  
AMPK

## ABSTRACT

Studies of the AMPK/PGC-1 $\alpha$  signaling pathway and exercise-induced metabolism have facilitated the development of anti-fatigue agents and exercise mimetics. In this work, adenosine and its 22 derivatives, typical of substitutions at the hydroxyl group of the sugar moiety, were firstly evaluated as anti-fatigue agents. In the running wheel tests, adenosine and most derivatives demonstrated a significant increase in the exhaustion distance when compared to the control group. Particularly, the optimized compound 2 exhibited a 3.1-fold increase in exhaustion distance compared to the positive control group treated with AICAR, and a remarkable 9.8-fold increase compared to the blank control group. Furthermore, improved performances were observed in weight-loaded swimming, high jumping, hanging wire, and tail suspension tests. Compound 2 not only reduced levels of lactic acid (LA) and blood urea nitrogen (BUN), but also preserved hepatic and muscle glycogen content during exercise. Notably, compound 2 activated AMPK/PGC-1 $\alpha$  pathway without stimulating the central nervous system. Moreover, compound 2 demonstrated a favorable safety *in vivo* at a dose of  $1.96 \times 10^{-5}$  mol/kg for 21 days. This study unveils, for the first time, the ability of adenosine and its derivatives to resist exercise-induced fatigue, thereby providing promising lead compounds for the development of drugs aimed to prevent and treat fatigue-related diseases. Moreover, it sheds light on the potential therapeutic approaches utilizing endogenous substance.

## 1. Introduction

Adenosine monophosphate-activated protein kinase (AMPK) plays a key role in the regulation of energy metabolism and is highly conserved from yeast to higher plants and animals. It is a heterotrimeric enzyme comprised of a highly conserved catalytic  $\alpha$ , a regulatory  $\beta$  and  $\gamma$  subunits (Lin and Hardie, 2018). Phosphorylated AMPK (p-AMPK) modulates sub-signaling proteins such as peroxisome proliferator-activated receptor  $\gamma$  coactivator-1 $\alpha$  (PGC-1 $\alpha$ ), thereby affecting protein synthesis, mitochondrial biogenesis, and fatty acid uptake in striated myocytes. PGC-1 $\alpha$  activation also promotes the expression of antioxidant-related genes (e.g., the superoxide dismutase gene family). Furthermore, the AMPK signaling pathway contributed to inducing skeletal muscle fiber type conversion from fast-twitch to slow-twitch to enhance exercise endurance (Yoon et al., 2019, Xu et al., 2020, Wen et al., 2021, Li et al.,

2022, Wu et al., 2022, Zhang et al., 2023).

Many dietary supplements, natural and synthetic molecules upregulate the AMPK/PGC-1 $\alpha$  pathway, thereby attenuating fatigue (Luo et al., 2019, Hu et al., 2020, Li et al., 2021, Zhu et al., 2021, Liu et al., 2022, Guo et al., 2023, Hu et al., 2023). Anti-fatigue agents have the potential to prevent and treat fatigue-related mental and physical health disorders, such as anxiety, depression, cognitive impairment, endocrinopathies, immunopathies and end-organ diseases (Cui et al., 2020, Wang et al., 2020, Chen et al., 2021, Peng et al., 2021, Peng et al., 2022). Because physical exercise activates AMPK to regulate mitochondrial biogenesis and energy metabolism, and since AMPK agonists promote many exercise-induced biochemical and functional effects, AMPK pathways are proposed as therapeutic targets for the development of "exercise mimetics" to confer the physiologic benefits of exercise without requiring muscle activity (Weihrauch and Handschin, 2018,

Peer review under responsibility of King Saud University.

\* Corresponding authors.

E-mail addresses: [zhangap1@163.com](mailto:zhangap1@163.com) (A. Zhang), [shiwg1988@126.com](mailto:shiwg1988@126.com) (W. Shi), [wj24998@163.com](mailto:wj24998@163.com) (L. Xu).

<sup>1</sup> These two authors contributed equally to this study.

<https://doi.org/10.1016/j.arabjc.2023.105490>

Received 21 March 2023; Accepted 26 November 2023

Available online 28 November 2023

1878-5352/© 2023 The Author(s). Published by Elsevier B.V. on behalf of King Saud University. This is an open access article under the CC BY-NC-ND license (<http://creativecommons.org/licenses/by-nc-nd/4.0/>).

Norikura et al., 2020, Ericsson et al., 2021, Spaulding and Yan, 2022). Exercise mimetics may offer medical alternatives to prevent and treat the complications of sedentariness that include obesity, metabolic syndrome, and cardiovascular disease; and to benefit patients with exercise intolerance due to paralysis, muscle dystrophy, cardiovascular disorders, morbid obesity, or other maladies.

Adenosine is a ubiquitous endogenous nucleoside that regulates a variety of neurobiological functions. To our knowledge, little research has been conducted regarding its potential application as an anti-fatigue agent. The accumulation of adenosine in brain tissue may act on the A1 receptor to inhibit hypocretin/orexin neurons in the lateral hypothalamus, consequently resulting in fatigue and sleep induction (Liu and Gao, 2007). However, adenosine can be phosphorylated to adenosine monophosphate (AMP) by adenosine kinase *in vivo*, raising the hypothesis that the systemic administration of adenosine may mitigate fatigue by activating AMPK. To assess this hypothesis, adenosine and its derivatives, which are characterized by substitution at the hydroxyl group of the sugar moiety, were evaluated for their potential as anti-fatigue agents. In total, 23 nucleosides were tested in murine models, and the optimal compound was subsequently investigated for safety and mechanism of action.

## 2. Materials and methods

### 2.1. Materials

The raw materials and reagents used in the synthesis experiment were obtained from Beijing InnoChem Science & Technology Co., Ltd. (Beijing, China). Lactic acid (LA), blood urea nitrogen (BUN), glycogen and lactate dehydrogenase (LDH) kits were obtained from Nanjing Jiancheng Bioengineering Institute (Nanjing, China). Insulin (INS) kit was obtained from Wuhan libori Biotechnology Co., Ltd (Wuhan, China). DMEM cell culture medium was purchased from Tianjin Bocheng Technology Co., Ltd. (Tianjin, China). Protein electrophoresis buffer was purchased from Sangon Biotech (Shanghai) Co., Ltd. (Shanghai, China). C2C12 myoblasts were obtained from Nanjing Kebai Biotechnology Co., Ltd (Nanjing, China). Anti-AMPK, anti-p-AMPK (Thr172), PGC-1 $\alpha$  antibodies and secondary antibodies conjugated with horseradish peroxidase IgG (rabbit and mouse) were purchased from Beijing ComWin Biotech Co., Ltd. (Beijing, China).

### 2.2. Chemical Synthesis Characterization

#### 2.2.1. 2',3'-O-isopropylidene adenosine (2)

*p*-Toluene sulfonic acid (32.93 g, 0.173 mol) and triethyl orthoformate (41 mL, 0.247 mol) were added to a solution of **1** (10 g, 0.037 mol) in acetone (1500 mL). The reaction mixture was stirred overnight at room temperature. After neutralization with saturated sodium carbonate, the solution was concentrated *in vacuo*, cooled for crystallization, and purified by column chromatography (CH<sub>2</sub>Cl<sub>2</sub>-MeOH, 10:1) to obtain **2** (11.4 g) (Zhang et al., 2015). Yield: 99.8%. <sup>1</sup>H NMR (400 MHz, DMSO-*d*<sub>6</sub>)  $\delta_{\text{H}}$  8.35 (s, 1H), 8.16 (s, 1H), 7.37 (s, 2H), 6.12 (d, *J* = 3.1 Hz, 1H), 5.36 (dd, *J* = 6.2, 3.1 Hz, 1H), 5.24 (dd, *J* = 6.0, 5.1 Hz, 1H), 4.96 (dd, *J* = 6.2, 2.5 Hz, 1H), 4.22 (td, *J* = 4.8, 2.5 Hz, 1H), 3.56 (qt, *J* = 10.4, 5.3 Hz, 2H), 1.56 (s, 3H), 1.35 (s, 3H); <sup>13</sup>C NMR (151 MHz, DMSO-*d*<sub>6</sub>)  $\delta_{\text{C}}$  156.36, 152.90, 149.05, 139.98, 119.32, 113.33, 89.90, 86.58, 83.47, 81.59, 61.83, 27.30, 25.41; MS (*m/z*): 308.13 [M + H]<sup>+</sup>.

#### 2.2.2. 2',3',5'-tri-O-acetyl-adenosine (3a)

Acetic anhydride (1.12 mL) was added to a solution of **1** (1 g, 0.0037 mol) in anhydrous pyridine (10 mL). The reaction mixture was stirred for 16 h at room temperature. The solution was quenched with EtOH (0.5 mL) and then concentrated three times *in vacuo* with 10 mL of toluene. The obtained yellowish oil was collected and purified by column chromatography (ethyl acetate-petroleum ether, 1:2) to obtain **3a** (0.81 g). Yield: 56.6%. <sup>1</sup>H NMR (400 MHz, DMSO-*d*<sub>6</sub>)  $\delta_{\text{H}}$  8.32 (s, 1H),

8.12 (s, 1H), 7.37 (s, 2H), 6.16 (d, *J* = 5.5 Hz, 1H), 5.99 (t, *J* = 5.7 Hz, 1H), 5.58 (dd, *J* = 5.9, 4.7 Hz, 1H), 4.41–4.33 (m, 1H), 4.31 (dd, *J* = 5.1, 3.8 Hz, 1H), 4.19 (dd, *J* = 11.7, 5.5 Hz, 1H), 2.07 (s, 2H), 1.98 (d, *J* = 11.1 Hz, 7H); <sup>13</sup>C NMR (151 MHz, DMSO-*d*<sub>6</sub>)  $\delta_{\text{C}}$  171.25, 170.63, 170.43, 156.53, 153.56, 149.58, 141.04, 119.64, 86.63, 80.00, 72.63, 70.56, 63.26, 21.05, 20.90, 20.76; MS (*m/z*): 394.14 [M + H]<sup>+</sup>.

#### 2.2.3. 2',3',5'-tri-O-tetra-propionyl-adenosine (3b)

**3b** synthesis was performed as previously described with some modifications (Nowak et al., 2005). Propionic anhydride (1.53 mL) was added to a solution of **1** (1 g, 0.0037 mol) in anhydrous pyridine (10 mL). The reaction mixture was stirred for 6 h at room temperature. The solution was quenched with EtOH (0.8 mL) and then concentrated three times *in vacuo* with 10 mL of toluene. The obtained yellowish oil was collected and purified by column chromatography (ethyl acetate-petroleum ether, 1:2) to obtain **3b** (0.77 g). Yield: 42.1%. <sup>1</sup>H NMR (400 MHz, DMSO-*d*<sub>6</sub>)  $\delta_{\text{H}}$  10.70 (s, 1H), 8.66 (d, *J* = 7.1 Hz, 2H), 6.32 (d, *J* = 5.2 Hz, 1H), 6.08 (t, *J* = 5.6 Hz, 1H), 5.69 (t, *J* = 5.3 Hz, 1H), 4.42 (td, *J* = 10.3, 8.8, 3.8 Hz, 2H), 4.28 (tt, *J* = 6.8, 2.6 Hz, 1H), 2.59 (q, *J* = 7.5 Hz, 2H), 2.42 (qt, *J* = 7.4, 3.6 Hz, 2H), 2.32 (dtd, *J* = 12.9, 7.4, 2.1 Hz, 4H), 1.12–1.05 (m, 6H), 0.99 (td, *J* = 7.5, 3.8 Hz, 6H); <sup>13</sup>C NMR (101 MHz, DMSO-*d*<sub>6</sub>)  $\delta_{\text{C}}$  173.30, 172.66, 172.50, 151.88, 151.40, 149.89, 143.18, 123.76, 85.95, 79.62, 72.03, 69.96, 62.66, 29.51, 26.63, 26.61, 26.44, 9.10, 8.84, 8.19, 8.71; MS (*m/z*): 492.21 [M + H]<sup>+</sup>.

#### 2.2.4. 2',3',5'-tri-O-propionyl-adenosine (3c)

Propionic anhydride (1.53 mL) was added to a solution of **1** (1 g, 0.0037 mol) in anhydrous pyridine (10 mL). The reaction mixture was stirred for 6 h at room temperature. The solution was quenched with EtOH (0.8 mL) and then concentrated three times *in vacuo* with 10 mL of toluene. The obtained yellowish oil was collected and purified by column chromatography (ethyl acetate-petroleum ether, 1:2) to obtain **3c** (0.85 g). Yield: 42.1%. <sup>1</sup>H NMR (400 MHz, DMSO-*d*<sub>6</sub>)  $\delta_{\text{H}}$  8.35 (s, 1H), 8.17 (s, 1H), 7.43 (s, 2H), 6.20 (d, *J* = 5.3 Hz, 1H), 6.04 (t, *J* = 5.6 Hz, 1H), 5.66 (t, *J* = 5.4 Hz, 1H), 4.42 (dd, *J* = 11.7, 3.7 Hz, 1H), 4.36 (q, *J* = 4.6 Hz, 1H), 4.26 (dd, *J* = 11.8, 5.3 Hz, 1H), 2.45–2.38 (m, 2H), 2.35–2.28 (m, 4H), 1.07 (t, *J* = 7.5 Hz, 3H), 0.99 (td, *J* = 7.4, 5.7 Hz, 6H); <sup>13</sup>C NMR (151 MHz, DMSO-*d*<sub>6</sub>)  $\delta_{\text{C}}$  173.30, 172.66, 172.50, 156.12, 152.77, 149.06, 140.04, 119.20, 85.68, 79.43, 71.92, 70.00, 62.71, 26.62, 26.59, 26.42, 8.87, 8.82, 8.74; MS (*m/z*): 436.19 [M + H]<sup>+</sup>.

#### 2.2.5. 2',3',5'-tri-O-tetra-butryl-adenosine (3d)

Butyric anhydride (1.94 mL) was added to a solution of **1** (1 g, 0.0037 mol) in anhydrous pyridine (10 mL). The reaction mixture was stirred for 6 h at room temperature. The solution was quenched with EtOH (1 mL) and then concentrated three times *in vacuo* with 10 mL of toluene. The obtained yellowish oil was collected and purified by column chromatography (ethyl acetate-petroleum ether, 1:2) to obtain **3d** (0.83 g). Yield: 45.3%. <sup>1</sup>H NMR (400 MHz, DMSO-*d*<sub>6</sub>)  $\delta_{\text{H}}$  10.71 (s, 1H), 8.64 (d, *J* = 6.0 Hz, 1H), 6.27 (d, *J* = 5.2 Hz, 1H), 6.05 (t, *J* = 5.6 Hz, 1H), 5.66 (t, *J* = 5.4 Hz, 1H), 4.37 (s, 1H), 3.42–3.33 (m, 2H), 3.28 (d, *J* = 3.4 Hz, 3H), 3.25 (s, 1H), 2.51 (d, *J* = 7.2 Hz, 2H), 2.44–2.15 (m, 6H), 1.51 (ddq, *J* = 47.2, 14.6, 7.4 Hz, 6H), 1.20 (s, 1H), 0.89 (q, *J* = 7.3 Hz, 3H), 0.78 (td, *J* = 7.4, 3.9 Hz, 4H); <sup>13</sup>C NMR (101 MHz, DMSO-*d*<sub>6</sub>)  $\delta_{\text{C}}$  175.79, 175.40, 174.98, 174.82, 166.74, 151.88, 151.44, 150.05, 143.13, 140.36, 130.79, 124.14, 86.09, 85.95, 79.63, 79.53, 72.16, 69.94, 62.60, 34.37, 33.10, 32.97, 19.20, 18.65, 18.63, 18.56, 18.50, 18.41; MS (*m/z*): 548.27 [M + H]<sup>+</sup>.

#### 2.2.6. 2',3',5'-tri-O-butryl-adenosine (3e)

Butyric anhydride (1.94 mL) was added to a solution of **1** (1 g, 0.0037 mol) in anhydrous pyridine (10 mL). The reaction mixture was stirred for 6 h at room temperature. The solution was quenched with EtOH (1 mL) and then concentrated three times *in vacuo* with 10 mL of toluene. The obtained yellowish oil was collected and purified by column chromatography (ethyl acetate-petroleum ether, 1:2) to obtain **3e**

(0.97 g). Yield: 54.3 %.  $^1\text{H}$  NMR (400 MHz, DMSO- $d_6$ )  $\delta_{\text{H}}$  8.31 (s, 1H), 8.12 (s, 1H), 7.37 (s, 2H), 6.16 (d,  $J = 5.3$  Hz, 1H), 6.02 (t,  $J = 5.6$  Hz, 1H), 5.67–5.60 (m, 1H), 4.38 (dd,  $J = 11.8, 3.7$  Hz, 1H), 4.32 (q,  $J = 4.7$  Hz, 1H), 4.22 (dd,  $J = 11.7, 5.2$  Hz, 1H), 2.43–2.15 (m, 5H), 1.56 (d,  $J = 7.3$  Hz, 1H), 1.56–1.48 (m, 1H), 1.46 (qd,  $J = 7.3, 5.6$  Hz, 4H), 1.20 (s, 1H), 0.89 (d,  $J = 7.4$  Hz, 2H), 0.85 (s, 1H), 0.88–0.74 (m, 6H);  $^{13}\text{C}$  NMR (101 MHz, DMSO- $d_6$ )  $\delta_{\text{C}}$  172.54, 171.86, 171.69, 156.20, 152.88, 149.14, 140.11, 119.25, 85.88, 79.57, 72.02, 70.04, 62.62, 35.18, 35.08, 34.92, 17.88, 17.82, 17.78, 13.36, 13.21; MS ( $m/z$ ): 478.52 [ $\text{M} + \text{H}$ ] $^+$ .

### 2.2.7. 2',3',5'-tri-*O*-tetra-isobutyryl-adenosine (3f)

Isobutyric anhydride (1.96 mL) was added to a solution of **1** (1 g, 0.0037 mol) in anhydrous pyridine (10 mL). The reaction mixture was stirred for 6 h at room temperature. The solution was quenched with EtOH (1 mL) and then concentrated three times *in vacuo* with 10 mL of toluene. The obtained yellowish oil was collected and purified by column chromatography (ethyl acetate-petroleum ether, 1:2) to obtain **3f** (0.97 g). Yield: 47.8 %.  $^1\text{H}$  NMR (400 MHz, DMSO- $d_6$ )  $\delta_{\text{H}}$  10.70 (s, 1H), 8.65 (d,  $J = 12.1$  Hz, 2H), 6.31 (d,  $J = 5.0$  Hz, 1H), 6.06 (t,  $J = 5.5$  Hz, 1H), 5.70 (t,  $J = 5.3$  Hz, 1H), 4.46–4.36 (m, 2H), 4.30 (dd,  $J = 11.8, 4.9$  Hz, 1H), 2.95 (p,  $J = 6.8$  Hz, 1H), 2.62 (ddd,  $J = 19.2, 13.2, 7.0$  Hz, 1H), 2.56–2.52 (m, 1H), 1.16–1.12 (m, 13H), 1.08–1.01 (m, 12H);  $^{13}\text{C}$  NMR (101 MHz, DMSO- $d_6$ )  $\delta_{\text{C}}$  172.42, 171.73, 171.58, 154.02, 151.85, 151.41, 150.08, 149.85, 148.67, 130.29, 123.86, 72.12, 71.95, 69.88, 62.48, 38.02, 35.08, 34.99, 34.82, 18.16, 17.80, 17.74, 17.69, 13.53, 13.33, 13.30, 13.18; MS ( $m/z$ ): 548.27 [ $\text{M} + \text{H}$ ] $^+$ .

### 2.2.8. 2',3',5'-tri-*O*-isobutyryl-adenosine (3g)

Isobutyric anhydride (1.96 mL) was added to a solution of **1** (1 g, 0.0037 mol) in anhydrous pyridine (10 mL). The reaction mixture was stirred for 6 h at room temperature. The solution was quenched with EtOH (1 mL) and then concentrated three times *in vacuo* with 10 mL of toluene. The obtained yellowish oil was collected and purified by column chromatography (ethyl acetate-petroleum ether, 1:2) to obtain **3g** (0.89 g). Yield: 50.2 %.  $^1\text{H}$  NMR (400 MHz, DMSO- $d_6$ )  $\delta_{\text{H}}$  8.33 (s, 1H), 8.15 (s, 1H), 7.38 (s, 2H), 6.20 (d,  $J = 5.0$  Hz, 1H), 6.02 (t,  $J = 5.4$  Hz, 1H), 5.68 (t,  $J = 5.3$  Hz, 1H), 4.41–4.36 (m, 2H), 4.28 (dd,  $J = 13.2, 6.2$  Hz, 1H), 2.62 (dt,  $J = 14.1, 7.1$  Hz, 1H), 2.57–2.53 (m, 1H), 1.14 (d,  $J = 7.0$  Hz, 7H), 1.05 (ddd,  $J = 13.4, 7.0, 4.2$  Hz, 12H);  $^{13}\text{C}$  NMR (101 MHz, DMSO- $d_6$ )  $\delta_{\text{C}}$  175.76, 174.96, 174.79, 156.09, 152.75, 149.01, 139.91, 119.16, 85.86, 79.40, 72.13, 69.97, 62.65, 33.10, 33.07, 32.95, 18.63, 18.61, 18.54, 18.50, 18.40; MS ( $m/z$ ): 478.23 [ $\text{M} + \text{H}$ ] $^+$ .

### 2.2.9. 2',3'-*O*-(3-methoxy-benzylidene)-adenosine (4a)

To a solution of **1** (1 g, 0.0037 mol) in anhydrous tetrahydrofuran (2 mL) was added zinc chloride anhydrous (3.5 g, 0.257 mol), add 3'-methoxybenzaldehyde (4 mL) under the protection of  $\text{N}_2$ . The reaction mixture was stirred for 24 h at room temperature. The solution was precipitated with ethyl acetate (20 mL), saturated sodium bicarbonate (6 mL) and then filtered. The organic layer was extracted with ethyl acetate (3  $\times$  30 mL). The combined organic layer was washed with water and concentrated *in vacuo*. The crude product was purified by column chromatography (ethyl acetate-petroleum ether, 1:2) to obtain **4a** (1.16 g). Yield: 80.5 %.  $^1\text{H}$  NMR (400 MHz, DMSO- $d_6$ )  $\delta_{\text{H}}$  8.38 (d,  $J = 2.6$  Hz, 1H), 8.17 (d,  $J = 2.2$  Hz, 1H), 7.37 (q,  $J = 9.7, 8.8$  Hz, 4H), 7.16–7.10 (m, 1H), 7.03 (dd,  $J = 19.7, 9.7$  Hz, 1H), 6.29 (dd,  $J = 4.9, 3.0$  Hz, 1H), 6.01 (s, 1H), 5.52–5.47 (m, 1H), 5.09 (d,  $J = 6.3$  Hz, 1H), 4.36 (t,  $J = 3.8$  Hz, 1H), 3.64–3.52 (m, 3H), 1.90 (s, 3H);  $^{13}\text{C}$  NMR (101 MHz, DMSO- $d_6$ )  $\delta_{\text{C}}$  156.15, 152.64, 148.78, 139.86, 137.69, 136.02, 130.39, 128.32, 127.39, 124.10, 119.11, 106.57, 89.39, 86.26, 83.78, 82.67, 61.51, 20.96; MS ( $m/z$ ): 386.15 [ $\text{M} + \text{H}$ ] $^+$ .

### 2.2.10. 2',3'-*O*-(3-methyl-benzylidene)-adenosine (4b)

To a solution of **1** (1 g, 0.0037 mol) in anhydrous tetrahydrofuran (2 mL) was added zinc chloride anhydrous (3.5 g, 0.257 mol), add 3'-

methylbenzaldehyde (3.9 mL) under the protection of  $\text{N}_2$ . The reaction mixture was stirred for 24 h at room temperature. The solution was precipitated with ethyl acetate (20 mL), saturated sodium bicarbonate (6 mL) and then filtered. The organic layer was extracted with ethyl acetate (3  $\times$  30 mL). The combined organic layer was washed with water and concentrated *in vacuo*. The crude product was purified by column chromatography (ethyl acetate-petroleum ether, 1:2) to obtain **4b** (0.75 g). Yield: 54.3 %.  $^1\text{H}$  NMR (400 MHz, DMSO- $d_6$ )  $\delta_{\text{H}}$  8.35 (d,  $J = 2.6$  Hz, 1H), 8.13 (d,  $J = 2.2$  Hz, 1H), 7.31 (m, 4H), 6.26 (dd,  $J = 19.7, 9.7$  Hz, 1H), 5.96 (s, 1H), 5.46 (dd,  $J = 4.9, 3.0$  Hz, 1H), 5.28 (m, 2H), 5.04 (dd,  $J = 6.3, 3.3$  Hz, 1H), 4.33 (m, 1H), 3.58 (m, 3H), 1.70 (s, 3H);  $^{13}\text{C}$  NMR (101 MHz, DMSO- $d_6$ )  $\delta_{\text{C}}$  156.16, 152.64, 148.79, 139.86, 137.70, 136.02, 130.39, 128.33, 127.39, 124.10, 119.11, 106.58, 89.39, 86.26, 83.78, 82.67, 61.52, 20.96; MS ( $m/z$ ): 370.17 [ $\text{M} + \text{H}$ ] $^+$ .

### 2.2.11. 2',3'-*O*-(*P*-methyl-benzylidene)-adenosine (4c)

To a solution of **1** (1 g, 0.0037 mol) in anhydrous tetrahydrofuran (2 mL) was added zinc chloride anhydrous (3.5 g, 0.257 mol), add *P*-methylbenzaldehyde (3.9 mL) under the protection of  $\text{N}_2$ . The reaction mixture was stirred for 24 h at room temperature. The solution was precipitated with ethyl acetate (20 mL), saturated sodium bicarbonate (6 mL) and then filtered. The organic layer was extracted with ethyl acetate (3  $\times$  30 mL). The combined organic layer was washed with water and concentrated *in vacuo*. The crude product was purified by column chromatography (ethyl acetate-petroleum ether, 1:2) to obtain **4c** (0.95 g). Yield: 65.9 %.  $^1\text{H}$  NMR (400 MHz, DMSO- $d_6$ )  $\delta_{\text{H}}$  8.38 (d,  $J = 2.6$  Hz, 1H), 8.27 (d,  $J = 2.2$  Hz, 1H), 7.37 (q,  $J = 9.7, 8.8$  Hz, 4H), 7.31–7.25 (m, 1H), 6.37 (dd,  $J = 19.7, 9.7$  Hz, 1H), 6.29 (dd,  $J = 4.9, 3.0$  Hz, 1H), 6.01 (s, 1H), 5.52–5.47 (m, 1H), 5.07 (dd,  $J = 6.5, 2.3$  Hz, 1H), 4.36 (t,  $J = 3.8$  Hz, 1H), 3.64–3.52 (m, 3H), 2.0 (s, 3H);  $^{13}\text{C}$  NMR (101 MHz, DMSO- $d_6$ )  $\delta_{\text{C}}$  156.14, 152.63, 148.78, 139.84, 139.28, 133.20, 128.95, 126.94, 124.24, 122.55, 119.09, 106.56, 89.44, 86.24, 83.71, 82.64, 61.51, 20.89; MS ( $m/z$ ): 370.14 [ $\text{M} + \text{H}$ ] $^+$ .

### 2.2.12. 2',3'-*O*-(3-fluoro-benzylidene)-adenosine (4d)

To a solution of **1** (1 g, 0.0037 mol) in anhydrous tetrahydrofuran (2 mL) was added zinc chloride anhydrous (3.5 g, 0.257 mol), add 3'-fluorobenzaldehyde (4.2 mL) under the protection of  $\text{N}_2$ . The reaction mixture was stirred for 24 h at room temperature. The solution was precipitated with ethyl acetate (20 mL), saturated sodium bicarbonate (6 mL) and then filtered. The organic layer was extracted with ethyl acetate (3  $\times$  30 mL). The combined organic layer was washed with water and concentrated *in vacuo*. The crude product was purified by column chromatography (ethyl acetate-petroleum ether, 1:2) to obtain **4d** (1.249 g). Yield: 89.4 %.  $^1\text{H}$  NMR (400 MHz, DMSO- $d_6$ )  $\delta_{\text{H}}$  8.40 (s, 1H), 8.16 (s, 1H), 7.61–7.40 (m, 4H), 7.47–7.35 (m, 1H), 6.30 (d,  $J = 2.8$  Hz, 1H), 6.01 (s, 1H), 5.50 (dd,  $J = 6.5, 2.8$  Hz, 1H), 5.32 (t,  $J = 5.5$  Hz, 1H), 5.07 (dd,  $J = 6.5, 2.3$  Hz, 1H), 4.34 (dt,  $J = 8.7, 5.2$  Hz, 3H), 3.56 (t,  $J = 3.8$  Hz, 1H), 3.51 (m, 3H);  $^{13}\text{C}$  NMR (101 MHz, DMSO- $d_6$ )  $\delta_{\text{C}}$  156.09, 152.69, 148.77, 140.01, 138.55, 133.22, 130.58, 129.84, 126.69, 125.79, 119.02, 105.44, 89.44, 86.34, 84.02, 82.90, 61.47; MS ( $m/z$ ): 374.12 [ $\text{M} + \text{H}$ ] $^+$ .

### 2.2.13. 2',3'-*O*-(3-chloro-benzylidene)-adenosine (4e)

To a solution of **1** (1 g, 0.0037 mol) in anhydrous tetrahydrofuran (2 mL) was added zinc chloride anhydrous (3.5 g, 0.257 mol), add 3'-chlorobenzaldehyde (4.2 mL) under the protection of  $\text{N}_2$ . The reaction mixture was stirred for 24 h at room temperature. The solution was precipitated with ethyl acetate (20 mL), saturated sodium bicarbonate (6 mL) and then filtered. The organic layer was extracted with ethyl acetate (3  $\times$  30 mL). The combined organic layer was washed with water and concentrated *in vacuo*. The crude product was purified by column chromatography (ethyl acetate-petroleum ether, 1:2) to obtain **4e** (1.145 g). Yield: 78.5 %.  $^1\text{H}$  NMR (400 MHz, DMSO- $d_6$ )  $\delta_{\text{H}}$  8.34 (s, 1H), 8.13 (s, 1H), 7.61 (q,  $J = 9.7, 8.8$  Hz, 3H), 7.52–7.47 (m, 1H), 7.37 (dd,  $J = 19.7, 9.7$  Hz, 1H), 6.19 (dd,  $J = 4.9, 3.0$  Hz, 1H), 6.01 (s, 1H), 5.51 (dd,

$J = 6.5, 2.8$  Hz, 1H), 5.21 (s, 1H), 5.08 (dd,  $J = 6.6, 2.4$  Hz, 1H), 4.34 (td,  $J = 5.1, 2.4$  Hz, 1H), 3.52 (tt,  $J = 11.5, 6.4$  Hz, 2H);  $^{13}\text{C}$  NMR (101 MHz, DMSO- $d_6$ )  $\delta_{\text{H}}$  156.09, 152.69, 148.76, 140.05, 138.54, 133.22, 130.57, 129.84, 126.68, 125.79, 119.00, 105.44, 89.45, 86.36, 84.03, 82.91, 61.48; MS ( $m/z$ ): 390.09 [M + H] $^{+}$ .

#### 2.2.14. 2',3'-O-(3-bromo-benzylidene)-adenosine (4f)

To a solution of 1 (1 g, 0.0037 mol) in anhydrous tetrahydrofuran (2 mL) was added zinc chloride anhydrous (3.5 g, 0.257 mol), add 3'-bromobenzaldehyde (4.1 mL) under the protection of  $\text{N}_2$ . The reaction mixture was stirred for 24 h at room temperature. The solution was precipitated with ethyl acetate (20 mL), saturated sodium bicarbonate (6 mL) and then filtered. The organic layer was extracted with ethyl acetate ( $3 \times 30$  mL). The combined organic layer was washed with water and concentrated in vacuo. The crude product was purified by column chromatography (ethyl acetate-petroleum ether, 1:2) to obtain 4f (0.981 g). Yield: 60.4 %.  $^1\text{H}$  NMR (400 MHz, DMSO- $d_6$ )  $\delta_{\text{H}}$  8.51 (s, 1H), 8.24 (s, 1H), 7.37 (m, 6H), 6.30 (d,  $J = 4.9, 3.0$  Hz, 1H), 6.01 (s, 1H), 5.52–5.47 (m, 1H), 5.08 (m, 1H), 4.40 (t,  $J = 3.8$  Hz, 1H), 3.56 (m, 2H);  $^{13}\text{C}$  NMR (101 MHz, DMSO- $d_6$ )  $\delta_{\text{H}}$  163.54, 161.12, 155.62, 152.88, 148.85, 141.31, 139.10, 139.03, 123.41, 123.39, 118.51, 117.08, 116.87, 105.71, 84.45, 83.17, 61.77. MS ( $m/z$ ): 434.02 [M + H] $^{+}$ .

### 2.3. Animals

Male Kunming (KM) mice (weighing 18–22 g each, five weeks old) were obtained from the Beijing Keyu Animal Breeding Center (Beijing, China; Permit number: SCXK (Jing) 2019–0010). Operational procedures were performed in accordance with the standards of the Guide for the Care and Use of Laboratory Animals published by the Institute of Laboratory Animal Resources of the National Research Council (USA). This study has received approval from the Animal Care and Use Committee of the Beijing Institute of Pharmacology and Toxicology. Best efforts were made to minimize the number of animals used and their suffering.

### 2.4. Drug Administration

5-aminimidazole-4-carboxamide nucleotide (AICAR) was used as a positive control, and its anti-fatigue effect through AMPK activation was verified (Narkar et al., 2008). Mice administrated 0.9 % sodium chloride (0.1 mL/mouse) constituted the blank control group. A single intraperitoneal injection of the drug and positive control substance ( $1.96 \times 10^{-5}$  mol/kg) was used based on literature (Zhu et al., 2022) and our past experience, and the test was performed 30 min after administration as the screening standard for the evaluation of compound activity.

### 2.5. Performance testing

#### 2.5.1. Running wheel test

Endurance testing was performed on a JY-YLS-10B mouse running wheel instrument (Shilian Boyan, Beijing, China). Exhaustion running distances were assessed according to the following procedure: 16 r/min for 15 min, 18 r/min for 5 min, 20 r/min for 5 min and 22 r/min for 5 min as an adaptive course before the test, followed by 24 r/min until exhaustion. Resting more than four times (30 s) within 60 min indicated exhaustion.

Evaluation was also conducted on mice receiving adaptive wheel training before testing: mice were acclimated to running (at speeds of 16 r/min for 15 min, 18 r/min for 5 min, 20 r/min for 5 min, 22 r/min for 5 min) five days prior to the test. All mice received drug or 0.9 % sodium chloride on the sixth day and were tested after the 30 min adaptation to assess exhaustion running distance.

#### 2.5.2. Weight-loaded swimming test

The mice were placed individually in a swimming pool (25 °C) and

loaded with a tin wire (6 % of body weight) on their tail root. The mice were considered exhausted when they did not rise to the surface of the water to breathe within 7 s (Liu et al., 2018).

#### 2.5.3. Hanging wire test

A thin line was hung on two iron frames, and the mice were placed on the thin line. The endurance of the mice was determined by observing the duration that their front and rear limbs held the thread. The time at which the mice fell off the thin line was recorded during the test.

#### 2.5.4. Tail suspension test

The tail suspension test was performed according to the reported method (Zhang et al., 2019). Briefly, mice were placed in a general soundproof behavior box and suspended 50 cm above the floor with tape placed approximately 1 cm from the tip of the tail. The total struggling time was recorded to indicate endurance. Mice that did not struggle for more than 15 s were considered exhausted.

#### 2.5.5. High jumping test

The water at the outer edge of a colorless water tank was heated to approximately 60 °C while the temperature at the bottom of the tank was maintained at 50 °C. The mice were stimulated to jump by the high water temperature. The average maximum jump height was measured to characterize explosive muscle strength.

### 2.6. Tissue collection and biochemical index

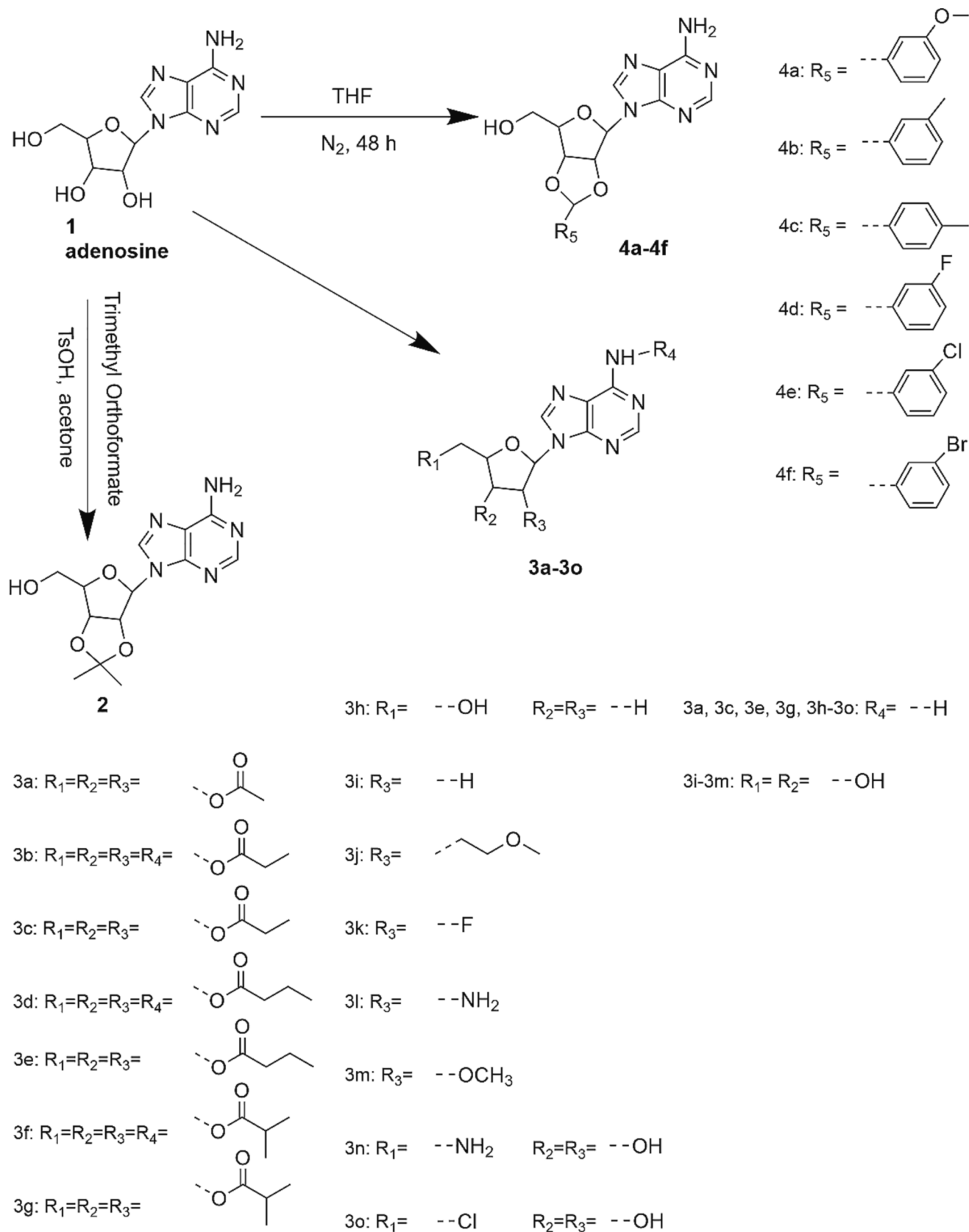
Blood samples were collected by *retro*-orbital puncture into EDTA capillary tubes for hematological and biochemical studies after the last exercise session. The mice were then sacrificed by cervical dislocation. The mice livers were harvested, and the gastrocnemius muscles of both hind legs were isolated, frozen and stored at  $-80$  °C until further analysis. Blood LA, BUN and glycogen levels were determined using the corresponding kits.

### 2.7. Western blot analysis

The C2C12 myoblasts were washed with cold PBS, then incubated with RIPA lysis buffer containing protease inhibitor cocktail and phosphatase inhibitor for 15 min and centrifuged at 1000 g and 4 °C for 8 min. Protein concentration was measured using a BCA assay kit. Equal amounts of sample proteins were separated by sodium dodecyl sulfate–polyacrylamide gel electrophoresis (SDS-PAGE) to analyze the proteins, which were compared with a protein marker (CWBI, Beijing, China). The proteins were transferred to a polyvinylidene fluoride (PVDF) membrane, and the membrane was blocked with 5 % skimmed milk powder in tris-buffered saline containing Tween 20 (TBST) for 1 h. After washing three times with TBST, the membrane was incubated in a solution containing primary antibody (AMPK, p-AMPK, PGC-1 $\alpha$ , and GAPDH antibodies, respectively) overnight at room temperature and visualized with horseradish peroxidase-coupled secondary antibody. Protein bands were detected using an enhanced chemiluminescence kit (CWBI, Beijing, China). An enhanced chemiluminescence western blot substrate (Pierce Biotechnology) was used for immunodetection, which was detected with the ChemiDoc™ MP Imaging System (Bio-Rad, USA). The bands were analyzed by densitometric analysis with the Image J software.

### 2.8. Open-field test

The test was conducted in a quiet environment. The mice were placed in the center of a closed plane area of a closed box divided into blocks, and their activities were measured by calculating the number of blocks traversed within 10 min. The movement of the animals was recorded by the camera and the total distance traveled by the mice under infrared light irradiation was automatically calculated by the



Scheme 1. Adenosine derivatives structure.

**Table 1**  
Compound purity and Log P value.

Compound	Log P	Purity
1	-1.17	99 %
2	-0.44	98 %
3a	-1.11	97 %
3b	1.22	99 %
3c	0.85	99 %
3d	2.89	99 %
3e	2.10	99 %
3f	3.48	99 %
3g	2.55	99 %
3h	-0.34	98 %
3i	-0.98	99 %
3j	-1.59	99 %
3k	-1.09	99 %
3l	-2.18	99 %
3m	-1.44	99 %
3n	-1.25	99 %
3o	-1.56	99 %
4a	0.73	96 %
4b	1.35	94 %
4c	1.35	97 %
4d	1.02	93 %
4e	1.42	95 %
4f	1.69	98 %

trajectory tracking method. This experiment was performed at 0.5 h and 3 h after administration.

## 2.9. Safety test

Male KM mice were divided randomly into two groups ( $n = 8$ ) and

treated by intraperitoneal injection for 21 days as follows: the blank control group (0.9 % sodium chloride, 0.1 mL/mouse) and the optimal compound group (2,  $1.96 \times 10^{-5}$  mol/kg/day). The mice were then sacrificed by cervical dislocation, and the heart, liver, spleen, lung, and kidney were collected and stained with hematoxylin and eosin for observation.

## 2.10. Cell culture and treatment

C2C12 myoblasts were cultured in DMEM containing 10 % fetal bovine serum at 37 °C and 5 % CO<sub>2</sub>. The C2C12 cells were induced to undergo myogenic differentiation with differentiation medium containing 2 % horse serum for 6 days. The cells were treated with 20 μM 2 or the solvent dimethyl sulfoxide.

## 2.11. Hematoxylin and eosin (H&E) staining

Hearts, livers, spleens, lungs, and kidneys were carefully collected and fixed in tissue fixative, dehydrated, embedded in paraffin, and cut into 5 μm thick sections. After deparaffinization, the tissue sections were rehydrated, stained with H&E, and subjected to morphological and pathological evaluation under a microscope.

## 2.12. Statistical analysis

All the experimental data were expressed as mean ± standard deviation. Significant differences were calculated using a two-tailed Student's *t*-test, and a *p*-value < 0.05 was considered statistically significant.

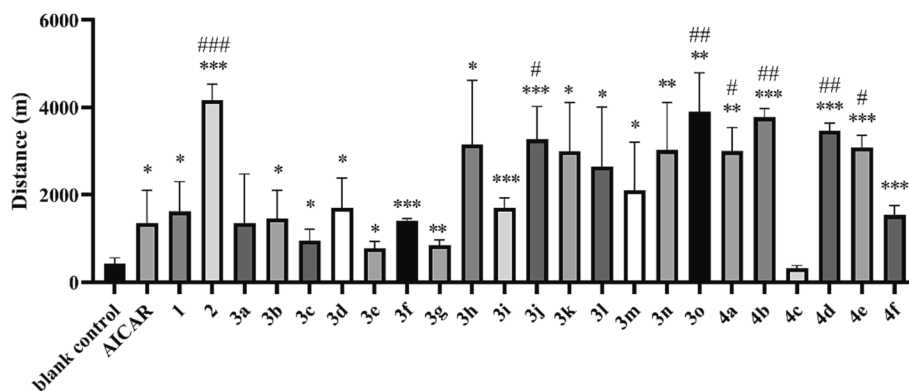


**Fig. 1.** Exhaustion distance of untrained mice in the running wheel test. \* $P < 0.05$ , \*\* $P < 0.01$ , \*\*\* $P < 0.001$  vs. the blank control group; # $P < 0.05$ , ## $P < 0.01$ , ### $P < 0.001$  vs. the AICAR group. Data are presented as the mean ± SD ( $n = 8$ ).

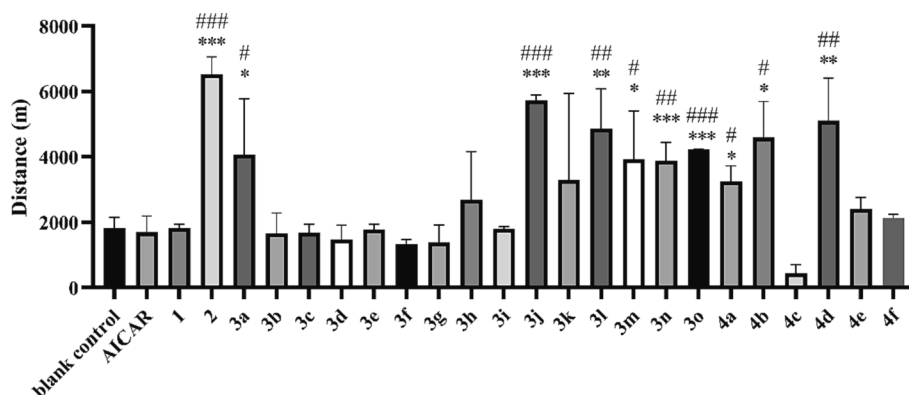


**Fig. 2.** Exhaustion distance of trained mice in the running wheel test. \* $P < 0.05$ , \*\* $P < 0.01$ , \*\*\* $P < 0.001$  vs. the blank control group; # $P < 0.05$ , ## $P < 0.01$ , ### $P < 0.001$  vs. the AICAR group. Data are presented as the mean ± SD ( $n = 8$ ).

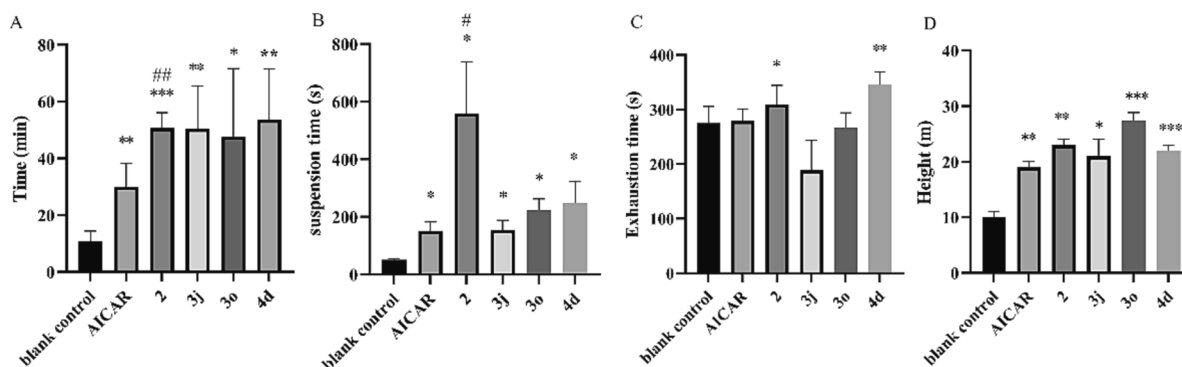


Fig. 3. A. Exhaustion time in the weight-loaded swimming test. B. Exhaustion time in the hanging wire test. C. Exhaustion time in the tail suspension test. D. Maximum jumping height in the high jumping test. \* $P < 0.05$ , \*\* $P < 0.01$ , \*\*\* $P < 0.001$  vs. the blank control group; # $P < 0.05$ , ## $P < 0.01$  vs. the AICAR group. Data are presented as the mean  $\pm$  SD ( $n = 8$ ).

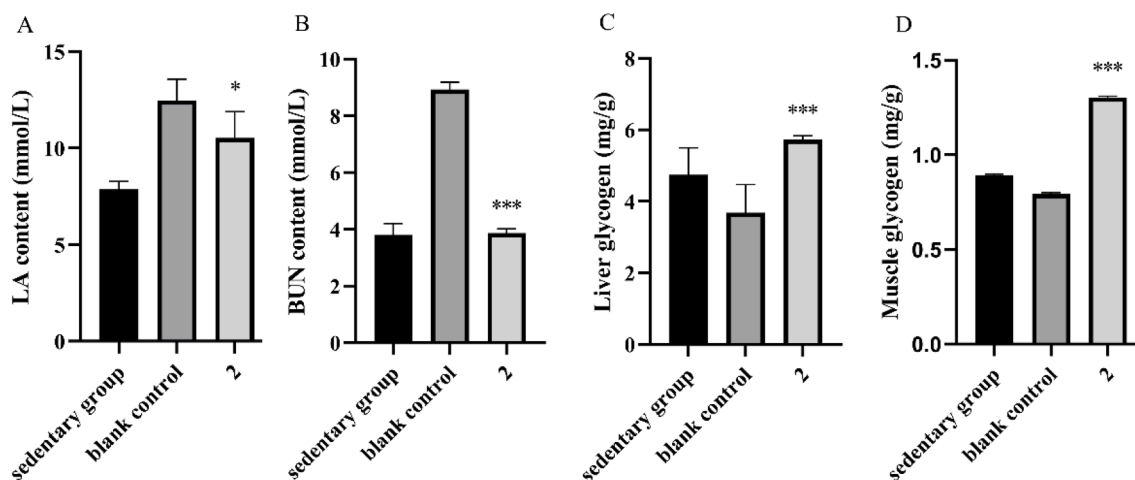


Fig. 4. Effect of 2 on the contents of (A) serum LA, (B) serum BUN, (C) liver glycogen and (D) muscle glycogen in mice. \* $P < 0.05$ , \*\*\* $P < 0.001$  vs. the blank control group. Data are presented as the mean  $\pm$  SD ( $n = 8$ ).

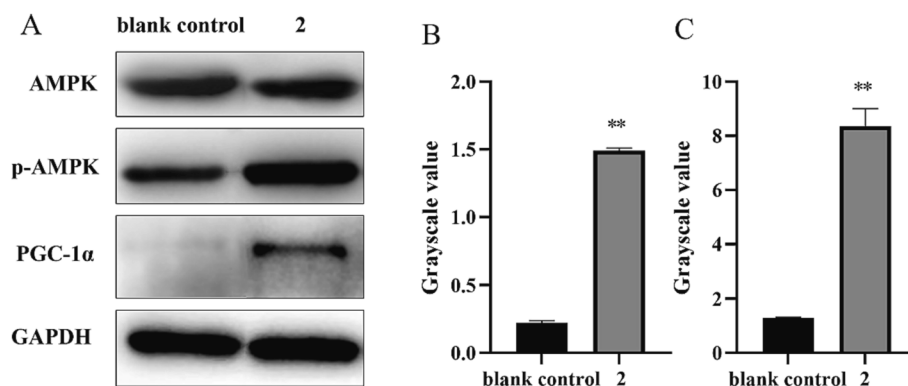


Fig. 5. (A) Western blot results for AMPK, p-AMPK, and PGC-1 $\alpha$ ; The gray values of p-AMPK/AMPK (B) and PGC-1 $\alpha$  (C) of 2. \*\* $P < 0.01$  vs. the blank control group.

### 3. Results and discussion

#### 3.1. Synthesis and Compounds

Fourteen adenosine derivatives (compound 2 to 3 g and 4) were synthesized from adenosine (compound 1) according to Scheme 1. The synthesis of the partial molecules was either based on pertinent literatures ((Nowak et al., 2005, van Wandelen et al., 2012, Zhang et al., 2015) or modified to optimize the synthesis process. The structures were

confirmed by  $^1\text{H}$  NMR,  $^{13}\text{C}$  NMR and MS. In addition, eight commercial derivatives (compounds 3 h to 3 o) were also included for evaluation. The purity of all compounds was determined by HPLC (Table 1).

Lipophilicity is important for drug delivery and activity. Adenosine is highly hydrophilic, with a Log P value of  $-1.17$  (predicted by Chem-Draw Ultra 8.0 software). After modification of the sugar moiety with different lipophilic substitutions, most target compounds exhibited higher Log P than adenosine, indicating improved lipophilicity.

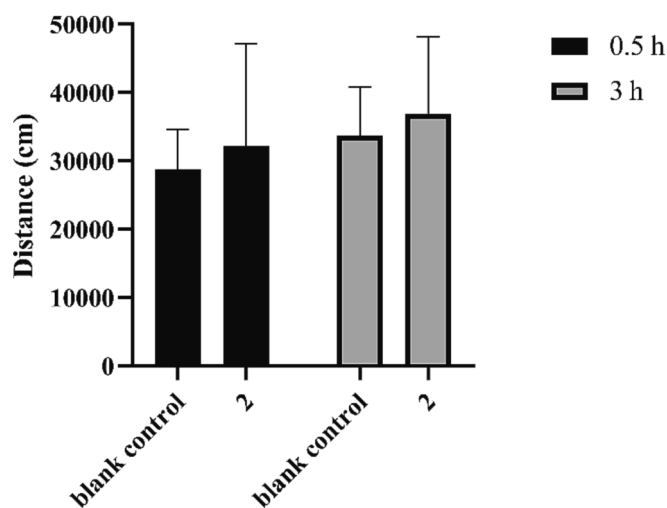


Fig. 6. Trajectory distances of mice in the open-field test. Data are expressed as the mean  $\pm$  SD ( $n = 8$ ).

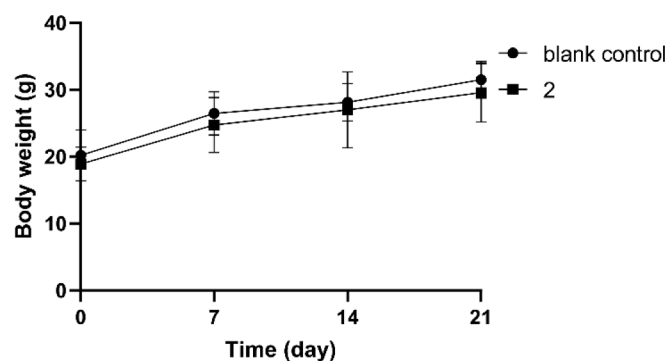


Fig. 7. Weight gain of mice during 21 days of administration. Data are expressed as mean  $\pm$  SD ( $n = 8$ ).

### 3.2. Activity evaluation by running wheel test

Running wheel tests of mice are commonly used to evaluate anti-fatigue agents. The longer the exhaustion distance, the better the molecular endurance improvement effect.

Adenosine attenuated fatigue as expected, the average exhaustion distance of the adenosine-treated group (1621.9 m) was significantly higher than that of blank control group (420.5 m,  $P < 0.05$ ) and was comparable to that of the AICAR group (1357.9 m,  $P > 0.05$ ). Most derivatives (compound **2**, **3b** to **4b**, **4d** to **4f**) enhanced fitness with significantly higher exhaustion distances than those of blank control

group (all  $P < 0.05$ ). Several derivatives (compound **2**, **3j**, **3o**, **4a**, **4b**, **4d**) outperformed AICAR group ( $P < 0.05$ ). The exhaustion distance of the most active derivative **2** (4162.0 m) was 3.1-fold higher than that of the AICAR group and 9.8-fold higher than that of the blank control group. To our knowledge, this was the first study to demonstrate that adenosine and its derivatives can resist exercise-induced fatigue (Fig. 1).

Evaluation was also carried out on mice that had undergone adaptive wheel training for 5 days prior to the test (referred to as “trained mice”). “Trained mice” provides an opportunity to further explore the efficiency of derivatives on potential object with good foundation of physical ability. Trained mice in the blank control group reached an average exhaustion distance of 1831.1 m, which was improved compared to that of the untrained blank control group (420.5 m), consistent with the axiom that exercise training improves physical endurance. Notably, the exhaustion distances of trained mice in AICAR (1695.3 m), adenosine (1828.2 m) and blank control groups were similar, indicating little anti-fatigue effect or physical fitness improvement for conditioned animals. However, several derivatives (compound **2**, **3j**, **3l**, **3n**, **3o**, **4a**, **4b**, **4d**) improved endurance significantly ( $P < 0.05$ ) and the performance of the **2** group (6529.4 m) was 3.6-fold higher than that of the blank control group (Fig. 2,  $P < 0.05$ ).

Our preliminary analysis of structure–activity relationship disclosed that 1) most derivatives with all the 2', 3', and 5' hydroxyl esterification (**3a** to **3g**) had lower endurance enhancing effects than those with cyclizing at the 2' and 3' hydroxyl site (compound **2** and compound **4**), indicating that the 5' hydroxyl was important for activity; 2) modification at 2' hydroxyl (**3i** to **3m**) might also enhance activity; 3) the performance of **3n** and **3o** suggested that replacing the 5' hydroxyl with chemically active groups might improve activity. Four derivatives (compound **2**, **3j**, **3o** and **4d**) associated with prolonged exhaustion distances above (Figure S1) were selected for further testing in anti-fatigue models.

### 3.3. Further evaluation of the activities of 2, 3j, 3o and 4d

The optimal molecules were further evaluated by weight-loaded swimming, tail suspension, hanging wire and high jumping tests.

The weight-loaded swimming test is also a common animal model for anti-fatigue evaluation. The weight-loaded swimming test disclosed that the average exhaustion times of the optimal compounds (50.7 min for **2**, 50.4 min for **3j**, 47.7 min for **3o**, 53.6 min for **4d** respectively) (Fig. 3A) were significantly longer than those of the blank control group (10.7 min,  $P < 0.05$ ). The results of the compound **2** group were even significantly higher than those of the AICAR group (30.0 min,  $P < 0.01$ ). The test was also conducted on mice subjected to a one-week pre-test adaptive training regimen. Swimming training improved the exhaustion time (Figure S2), as the blank control group improved from 10.7 min to 27.5 min after training. **2** also exhibited the best enhancement of exercise endurance (70.9 min), which was significantly longer than that of

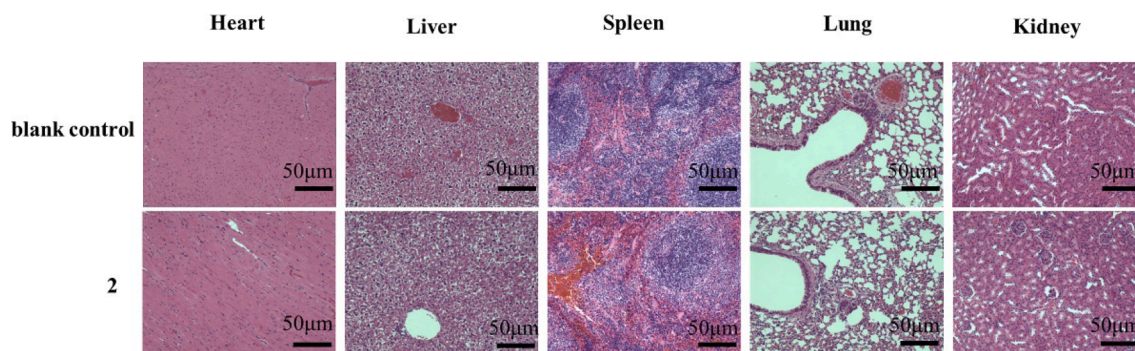


Fig. 8. H&E staining histological sections of heart, liver, spleen, lung and kidneys at 21 days after treatment of mice with **2** ( $1.96 \times 10^{-5}$  mol/kg/day) or 0.9 % sodium chloride (blank control). Images were taken with a Leica microscope. Magnification, 400  $\times$ . Scale bar = 50  $\mu$ m.

the AICAR group (38.4 min).

The hanging wire test can reflect the degree of grip endurance of the mouse limbs as well as their motor coordination capability. The hanging wire test revealed a longer suspension time in the **2** group than in the other groups (Fig. 3B). The tail suspension test reflects the escape-related behavior of mice subjected to a short-term inescapable stress (being suspended by their tails) (Wang et al., 2021). The tail suspension test disclosed similar struggle times in the AICAR and blank control groups, while the struggle times of the **2** (309.0 s) and **4d** (345.0 s) groups were higher than that of blank control group (275.0 s,  $P < 0.01$ ) (Fig. 3C). Moreover, very interestingly, these optimized compounds also improved external heat-stimulated jumping performance in the high jumping test, indicating their potential to improve explosive muscle strength (Fig. 3D).

According to the aforementioned results, compound **2** exhibited superior performance in two running wheel tests and the hanging wire test, with analogous activities observed in other tests relative to **3j**, **3o** and **4d**. Furthermore, our preliminary side effect assessment demonstrated a high accumulation of LA in **3o** administration and identified a potential cancer risk associated with **3j**. As a result, compound **2** was selected for further evaluation.

In a dose–response running wheel test, the exhaustion distance shortened with **2** dose reductions (Figure S3), indicating a dose-dependent activity. Moreover, the intragastric administration of **2** exerted a definite anti-fatigue effect ( $1.96 \times 10^{-5}$  mol/kg), suggesting the possibility of an oral drug delivery route (Figure S4). These results indicate that **2** enhanced the physiologic endurance of mice substantially. To our knowledge, **2** is one of the most potent anti-fatigue agents reported to date.

### 3.4. Biochemical Index Evaluation

Mice were trained for five days, then administered either compound **2** or 0.9 % sodium chloride and were sacrificed for biochemical assays after reaching 1500 m in the running wheel test. LA and BUN levels are commonly used to reflect the severity of fatigue. In our test, LA accumulation was greater in the blank control group after exercise than in the sedentary group. However, the LA level of **2** group was significantly lower than that of blank control group (Fig. 4A,  $P < 0.05$ ), indicating that animals in the **2** group were less fatigued. Furthermore, the mean LDH level of the **2** group was significantly higher than that of blank control group (Fig. S5A,  $P < 0.05$ ). LA is the primary metabolic waste product of anaerobic glycolysis during high-intensity exercise. Excessive LA accumulation causes muscle pain and acidosis, which is a major cause of fatigue. Reducing the buildup of LA also lowers the risk of muscle injury during exercise (Brooks, 2020). LDH is an endogenous enzyme of the glycolytic pathway that catalyzes a redox reaction between pyruvic acid and LA, thus playing an important role in LA clearance during intense exercise (Ye et al., 2017). In this study, **2** inhibited LA accumulation, thus providing a potential role in contributing to the postponement of fatigue, which is consistent with the results in our behavioral test.

The post-exercise BUN content in the blank control group was significantly higher than that of the sedentary group. However, the BUN content in the **2** group was significantly lower than that of the blank group (Fig. 4B,  $P < 0.05$ ), suggesting that animals in **2** group were less fatigued than the blank group. When the body is unable to obtain energy from carbohydrates and fats, proteins and amino acids become alternative sources of catabolism to meet energy requirements. An established marker of protein and amino acid catabolism is BUN. Therefore, an increase in BUN commonly reflects protein breakdown, which can jeopardize muscle contraction strength, thereby reducing endurance and increasing fatigue. (Zhu et al., 2021). In this study, **2** treatment significantly reduced BUN, indicating that **2** inhibited the accumulation of BUN, thereby postponing the occurrence of fatigue.

Glycogen is consumed through aerobic and anaerobic respiration,

thus providing energy necessary for exercise. Glycogen depletion lowers blood glucose concentration, resulting in hypoglycemia and fatigue (Feng et al., 2021). Therefore, glycogen content plays an important role in improving sports endurance and recovering sports fatigue (Ren et al., 2011). Post-exercise liver/muscle glycogen levels in the blank group were significantly lower than those in the sedentary group (Fig. 4C and 4D,  $P < 0.05$ ), due to consumption during exercise. However, liver/muscle glycogen levels in **2** group were significantly higher than those in the blank group ( $P < 0.01$ ). This result might have been related to the higher mean serum insulin level of the **2** than that of the blank control group (Fig. S5B), as INS regulates glucose uptake as well as glycogen synthesis and storage. Increased glycogen stores increase the intracellular bioavailability of glucose as a metabolic fuel, thereby, delaying the consumption of protein as an energy source, which might also explain why mice in the **2** exhibited lower BUN levels than the blank control group.

### 3.5. **2** enhanced AMPK/ PGC-1 $\alpha$ pathway

AMPK, as a key energy sensor, is a major regulator of energy homeostasis between cells and organisms. Western blot analysis was conducted in a C2C12 cell model. **2** significantly enhanced AMPK phosphorylation; p-AMPK/AMPK was increased relative to the blank group. The expression of a downstream factor, PGC-1 $\alpha$ , was also up-regulated significantly (Fig. 5).

A large number of studies have shown that the abnormal energy metabolism associated with exercise fatigue may be related to the AMPK/PGC-1 $\alpha$  pathway (Wang et al., 2021, Qu et al., 2022, Yu et al., 2023). Up-regulation of AMPK/PGC-1 $\alpha$  pathway significantly improves the energy supply of skeletal muscle and also promotes muscle fiber type transformation, glucose metabolism, and fatty acid oxidative metabolism, thus increasing muscle endurance and reducing fatigue (Narkar et al., 2008, Cantó and Auwerx, 2009). This is consistent with our results that **2** can upregulating the AMPK/PGC-1 $\alpha$  pathway to achieve its anti-fatigue effects.

### 3.6. Open-field test

An open field test was conducted to investigate whether **2** exerted a central stimulant effect. At 0.5 h and 3 h after administration, the total distance traversed by treated mice within 10 min was not significantly different from that of the blank control group (Fig. 6), indicating that **2** did not excite spontaneous movement. Thus, **2** had no central stimulation in mice, which proved that **2** did not exert anti-fatigue activity through an excitatory effect on the central nervous system.

### 3.7. Safety of **2**

The safety of **2** was evaluated in mice receiving intraperitoneal injections ( $1.96 \times 10^{-5}$  mol/kg/d) for 21 days. Body weight increased normally during the test interval, without obvious abnormalities by daily observation (Fig. 7). In addition, tissue sections of sampled heart, liver, spleen, lung, and kidney observed by hematoxylin and eosin staining showed no obvious inflammation or injuries (Fig. 8). These results indicate good *in vivo* safety of **2**.

## 4. Conclusion

In summary, the present study evaluated adenosine and its 22 derivatives as potential anti-fatigue agents. To our knowledge, we report the first demonstration of the enhancement of exercise performance in mice treated with adenosine or several lipophilic derivatives. Of the evaluated compounds, an optimal compound **2** was found to exhibit outstanding anti-fatigue activity. The underlying mechanisms of action included reduction in LA and BUN levels, as well as increased hepatic and muscle glycogen content. Compound **2** was found to enhance the

AMPK/PGC-1 $\alpha$  pathway, without causing central nervous system excitation. Based on these findings, Compound 2 may represent an ideal candidate for the development and utilization of novel anti-fatigue drug and exercise mimetics, which could offer new therapeutic approaches for the prevention and treatment of AMPK-related diseases, such as obesity, type 2 diabetes, and cardiovascular disease. This study also sheds light on the potential therapeutic interventions utilizing endogenous substance.

#### CRedit authorship contribution statement

**Huimin Zhu:** Conceptualization, Investigation, Writing – original draft. **Tangna Zhao:** Investigation, Writing – original draft. **Wanbo Zeng:** Conceptualization. **Xiao Dong:** Investigation, Formal analysis. **Yuan Luo:** Investigation, Formal analysis. **Xiang Li:** Investigation, Formal analysis. **Aiping Zhang:** Investigation, Formal analysis. **Weiguo Shi:** Project administration. **Liang Xu:** Supervision, Project administration, Funding acquisition.

#### Declaration of competing interest

The authors declare that they have no known competing financial interests or personal relationships that could have appeared to influence the work reported in this paper.

#### Acknowledgement

This work was supported by the Beijing Nova Program (20220484229).

#### Appendix A. Supplementary material

Supplementary data to this article can be found online at <https://doi.org/10.1016/j.arabjc.2023.105490>.

#### References

- Brooks, G.A., 2020. Lactate as a fulcrum of metabolism. *Redox Biol.* 35, 101454 <https://doi.org/10.1016/j.redox.2020.101454>.
- Cantó, C., Auwerx, J., 2009. PGC-1 $\alpha$ , SIRT1 and AMPK, an energy sensing network that controls energy expenditure. *Curr. Opin. Lipidol.* 20, 98–105. <https://doi.org/10.1097/MOL.0b013e328328d0a4>.
- Chen, Y.J., Kuo, C.Y., Kong, Z.L., et al., 2021. Anti-fatigue effect of a dietary supplement from the fermented by-products of taiwan tilapia aquatic waste and Monostroma nitidum oligosaccharide complex. *Nutrients* 13. <https://doi.org/10.3390/n13051688>.
- Cui, J., Xia, P., Zhang, L., et al., 2020. A novel fermented soybean, inoculated with selected *Bacillus*, *Lactobacillus* and *Hansenula* strains, showed strong antioxidant and anti-fatigue potential activity. *Food Chem.* 333, 127527 <https://doi.org/10.1016/j.foodchem.2020.127527>.
- Ericsson, M., Steneberg, P., Nyrén, R., et al., 2021. AMPK activator O304 improves metabolic and cardiac function, and exercise capacity in aged mice. *Commun. Biol.* 4, 1306. <https://doi.org/10.1038/s42003-021-02837-0>.
- Feng, T., Huang, Y., Tang, Z., et al., 2021. Anti-fatigue effects of pea (*Pisum sativum* L.) peptides prepared by compound protease. *J. Food Sci. Technol.* 58, 2265–2272. <https://doi.org/10.1007/s13197-020-04737-3>.
- Guo, J., Yan, E., He, L., et al., 2023. Dietary supplementation with lauric acid improves aerobic endurance in sedentary mice via enhancing fat mobilization and glyconeogenesis. *J. Nutr.* 153, 3207–3219. <https://doi.org/10.1016/j.tjnut.2023.09.006>.
- Hu, M., Du, J., Du, L., et al., 2020. Anti-fatigue activity of purified anthocyanins prepared from purple passion fruit (*P. edulis* Sim) epicarp in mice. *J. Funct. Foods* 65, 103725. <https://doi.org/10.1016/j.jff.2019.103725>.
- Hu, M., Han, M., Zhang, H., et al., 2023. Curcumin (CUMINUP60®) mitigates exercise fatigue through regulating PI3K/Akt/AMPK/mTOR pathway in mice. *Aging* 15, 2308–2320. <https://doi.org/10.18632/aging.204614>.
- Li, H., Chen, X., Huang, Z., et al., 2022. Ellagic acid enhances muscle endurance by affecting the muscle fiber type, mitochondrial biogenesis and function. *Food Funct.* 13, 1506–1518. <https://doi.org/10.1039/d1fo02318g>.
- Li, M., Tian, X., Li, X., et al., 2021. Anti-fatigue activity of gardenia yellow pigment and Cistanche phenylethanol glycosides mixture in hypoxia. *Food Biosci.* 40, 100902. <https://doi.org/10.1016/j.fbio.2021.100902>.
- Lin, S.C., Hardie, D.G., 2018. AMPK: Sensing glucose as well as cellular energy status. *Cell Metab.* 27, 299–313. <https://doi.org/10.1016/j.cmet.2017.10.009>.
- Liu, Z.W., Gao, X.B., 2007. Adenosine inhibits activity of hypocretin/orexin neurons by the A1 receptor in the lateral hypothalamus: a possible sleep-promoting effect. *J. Neurophysiol.* 97, 837–848. <https://doi.org/10.1152/jn.00873.2006>.
- Liu, S., Meng, F., Zhang, D., et al., 2022. Lonicera caerulea berry polyphenols extract alleviates exercise fatigue in mice by reducing oxidative stress, inflammation, skeletal muscle cell apoptosis, and by increasing cell proliferation. *Front. Nutr.* 9, 853225 <https://doi.org/10.3389/fnut.2022.853225>.
- Liu, R., Wu, L., Du, Q., et al., 2018. Small molecule oligopeptides isolated from walnut (*Juglans regia* L.) and their anti-fatigue effects in mice. *Molecules (Basel Switzerland)* 24, 45. <https://doi.org/10.3390/molecules24010045>.
- Luo, C., Xu, X., Wei, X., et al., 2019. Natural medicines for the treatment of fatigue: Bioactive components, pharmacology, and mechanisms. *Pharmacol. Res.* 148, 104409 <https://doi.org/10.1016/j.phrs.2019.104409>.
- Narkar, V.A., Downes, M., Yu, R.T., et al., 2008. AMPK and PPAR $\delta$  agonists are exercise mimetics. *Cell* 134, 405–415. <https://doi.org/10.1016/j.cell.2008.06.051>.
- Norikura, T., Kajiyama, S., Sugawara, M., et al., 2020. cis-Banglene, a bangle (Zingiber purpureum)-derived bioactive compound, promotes mitochondrial biogenesis and glucose uptake by activating the IL-6/AMPK signaling pathway in C2C12 skeletal muscle cells. *J. Funct. Foods* 64, 103632. <https://doi.org/10.1016/j.jff.2019.103632>.
- Nowak, I., Conda-Sheridan, M., Robins, M.J., 2005. Nucleic acid related compounds. 127. Selective N-deacylation of N, O-peracetylated nucleosides in superheated methanol. *J. Org. Chem.* 70, 7455–7458. <https://doi.org/10.1021/jo051256w>.
- Peng, F., Yin, H., Du, B., et al., 2021. Anti-fatigue activity of purified flavonoids prepared from chestnut (*Castanea mollissima*) flower. *J. Funct. Foods* 79, 104365. <https://doi.org/10.1016/j.jff.2021.104365>.
- Peng, Y., Zhao, L., Hu, K., et al., 2022. Anti-fatigue effects of Lycium barbarum polysaccharide and effervescent tablets by regulating oxidative stress and energy metabolism in rats. *Int. J. Mol. Sci.* 23 <https://doi.org/10.3390/ijms231810920>.
- Qu, Y., Ji, H., Song, W., et al., 2022. The anti-fatigue effect of the Auxis thazard oligopeptide via modulation of the AMPK/PGC-1 $\alpha$  pathway in mice. *Food Funct.* 13, 1641–1650. <https://doi.org/10.1039/d1fo03320d>.
- Ren, J., Zhao, M., Wang, H., et al., 2011. Effects of supplementation with grass carp protein versus peptide on swimming endurance in mice. *Nutrition (Burbank, Los Angeles County, Calif.)* 27, 789–795. <https://doi.org/10.1016/j.nut.2010.08.020>.
- Spaulding, H.R., Yan, Z., 2022. AMPK and the adaptation to exercise. *Annu. Rev. Physiol.* 84, 209–227. <https://doi.org/10.1146/annurev-physiol-060721-095517>.
- van Wandelen, L.T., van Ameijde, J., Mady, A.S., et al., 2012. Directed modulation of protein kinase C isozyme selectivity with bisubstrate-based inhibitors. *ChemMedChem* 7, 2113–2121. <https://doi.org/10.1002/cmdc.201200349>.
- Wang, P., Zeng, H., Lin, S., et al., 2020. Anti-fatigue activities of hairtail (*Trichiurus lepturus*) hydrolysate in an endurance swimming mice model. *J. Funct. Foods* 74, 104207. <https://doi.org/10.1016/j.jff.2020.104207>.
- Wang, P., Wang, D., Hu, J., et al., 2021. Natural bioactive peptides to beat exercise-induced fatigue: A review. *Food Biosci.* 43, 101298 <https://doi.org/10.1016/j.fbio.2021.101298>.
- Wang, Z., Xia, T., Jin, S., et al., 2021. Chronic restraint stress-induced muscle atrophy leads to fatigue in mice by inhibiting the AMPK signaling pathway. *Biomedicine* 9. <https://doi.org/10.3390/biomedicine9101321>.
- Weihrauch, M., Handschin, C., 2018. Pharmacological targeting of exercise adaptations in skeletal muscle: Benefits and pitfalls. *Biochem. Pharmacol.* 147, 211–220. <https://doi.org/10.1016/j.bcp.2017.10.006>.
- Wen, W., Chen, X., Huang, Z., et al., 2021. Lycopene increases the proportion of slow-twitch muscle fiber by AMPK signaling to improve muscle anti-fatigue ability. *J. Nutr. Biochem.* 94, 108750 <https://doi.org/10.1016/j.jnutbio.2021.108750>.
- Wu, L., Zhou, M., Li, T., et al., 2022. GLP-1 regulates exercise endurance and skeletal muscle remodeling via GLP-1R/AMPK pathway. *Biochimica et Biophysica Acta. Mol. Cell Res.* 1869, 119300 <https://doi.org/10.1016/j.bbamer.2022.119300>.
- Xu, M., Chen, X., Huang, Z., et al., 2020. Procyranidin B2 promotes skeletal slow-twitch myofiber gene expression through the AMPK signaling pathway in C2C12 myotubes. *J. Agric. Food Chem.* 68, 1306–1314. <https://doi.org/10.1021/acs.jafc.9b07489>.
- Ye, J., Shen, C., Huang, Y., et al., 2017. Anti-fatigue activity of sea cucumber peptides prepared from *Stichopus japonicus* in an endurance swimming rat model. *J. Sci. Food Agric.* 97, 4548–4556. <https://doi.org/10.1002/jsfa.8322>.
- Yoon, K.J., Zhang, D., Kim, S.J., et al., 2019. Exercise-induced AMPK activation is involved in delay of skeletal muscle senescence. *Biochem. Biophys. Res. Commun.* 512, 604–610. <https://doi.org/10.1016/j.bbrc.2019.03.086>.
- Yu, Y., Nie, J., Zhao, B., et al., 2023. Structure characterization and anti-fatigue activity of an acidic polysaccharide from Panax ginseng C. A. Meyer. *J. Ethnopharmacol.* 301, 115831 <https://doi.org/10.1016/j.jep.2022.115831>.
- Zhang, X., Jing, S., Lin, H., et al., 2019. Anti-fatigue effect of anwulignan via the NRF2 and PGC-1 $\alpha$  signaling pathway in mice. *Food Funct.* 10, 7755–7766. <https://doi.org/10.1039/c9fo01182j>.
- Zhang, J., Li, J., Liu, Y., et al., 2023. Effect of resveratrol on skeletal slow-twitch muscle fiber expression via AMPK/PGC-1 $\alpha$  signaling pathway in bovine myotubes. *Meat Sci.* 204, 109287 <https://doi.org/10.1016/j.meatsci.2023.109287>.
- Zhang, G., Richardson, S.L., Mao, Y., et al., 2015. Design, synthesis, and kinetic analysis of potent protein N-terminal methyltransferase 1 inhibitors. *Org. Biomol. Chem.* 13, 4149–4154. <https://doi.org/10.1039/c5ob00120j>.

Zhu, S., Yang, W., Lin, Y., et al., 2021. Antioxidant and anti-fatigue activities of selenium-enriched peptides isolated from Cardamine violifolia protein hydrolysate. *J. Funct. Foods* 79, 104412. <https://doi.org/10.1016/j.jff.2021.104412>.

Zhu, J., Yi, J., Kang, Q., et al., 2021. Anti-fatigue activity of hemp leaves water extract and the related biochemical changes in mice. *Food Chem. Toxicol.* 150, 112054 <https://doi.org/10.1016/j.fct.2021.112054>.

Zhu, H., Zeng, W., Zhao, T., et al., 2022. Synthesis and evaluation of 5-aminimidazole-4-carboxamide riboside derivatives as anti-fatigue agents. *Arab. J. Chem.* 15, 104313 <https://doi.org/10.1016/j.arabjc.2022.104313>.